Fabrication and molecular beam epitaxy regrowth of first-order, high contrast AlGaAs/GaAs gratings

C. S. Wang,[a] G. B. Morrison, E. J. Skogen, and L. A. Coldren
Department of Electrical and Computer Engineering, University of California, Santa Barbara, California 93106

(Received 14 September 2005; accepted 2 January 2006; published 30 May 2006)

We present a fabrication technique and molecular beam epitaxy (MBE) regrowth of first-order, high contrast AlGaAs/GaAs diffraction gratings for laser emitting at 980 nm. An immersion holography technique is used to uniformly pattern first-order gratings with a pitch of 155 nm. MBE is used to overgrow $Al_{0.75}Ga_{0.25}As$ on etched GaAs gratings. It is found that slow growth rates with optimum arsenic overpressure are necessary to overgrow gratings with low pitting defect densities. These first-order, high contrast gratings are integrated as distributed Bragg reflectors in an edge-emitting laser structure. Single-mode emission at 1 μm with a side mode suppression ratio greater than 30 dB is demonstrated. © *2006 American Vacuum Society.* [DOI: 10.1116/1.2190679]

I. INTRODUCTION

Photonic integrated circuits are providing a solution to the growing demands for low-cost optoelectronics with increased device functionality and improved performance. With lower costs and improved performance, applications for photonic integrated circuits are emerging. For instance, high-efficiency, short-cavity transmitters have recently been developed as part of an optical solution to the growing bandwidth and path-length requirements of chip to chip optical interconnects.[1] These edge-emitting transmitters have higher output powers and bandwidths than conventional vertical-cavity lasers and are therefore able to drive "receiverless" architectures. To accommodate the high power, high-efficiency, and high temperature specifications of an optical interconnect, transmitters operating at a wavelength of 980 nm were fabricated on GaAs.[2]

A key component within these integrated 980 nm transmitters is the distributed Bragg reflector (DBR), which enables single-frequency operation. Fabrication of DBRs for lasers based at 980 nm or shorter wavelengths on GaAs is challenging due to the shorter grating pitch compared to conventional 1550 nm DBRs on InP. For 980 nm DBRs, higher order gratings are used, but these higher order gratings suffer from lower coupling coefficients, larger footprints, and increased loss.[3] Surface gratings and deeply etched gratings have also been used; these take advantage of the large index of refraction difference between semiconductor and air but require very smooth and precise etching techniques and have increased scattering and diffraction losses.[4,5]

In this work, we present an immersion holography technique for the fabrication of first-order gratings. Regrowth over the gratings is accomplished by molecular beam epitaxy (MBE). There have been a few reports of using MBE to regrow gratings, but these generally involve higher order gratings and use lower contrast AlGaAs ($x<0.45$), resulting in a lower grating coupling coefficient κ.[6–8] In order to maximize κ, $Al_{0.75}Ga_{0.25}As$ was overgrown for the realization of strong reflectors with small footprint. The quality of the regrown gratings was studied by varying the growth rate and growth temperatures and evaluated using atomic force microscopy (AFM) and scanning electron microscopy (SEM). These first-order AlGaAs/GaAs DBRs were then successfully integrated into an edge-emitting laser structure.

II. HOLOGRAPHY

We have chosen to use holography over direct e-beam writing to pattern gratings due to advantages of cost, throughput, and simplicity. Figure 1 shows a diagram of the setup. In our holography setup, a HeCd laser emitting at 325 nm is used as the source. The beam is expanded through a pinhole and is incident on a rotational stage consisting of the sample and an optical mirror. The reflection from the mirror creates a standing wave pattern which exposes the photoresist on the sample surface in a spatially periodic manner. The resulting grating pitch Λ is controlled by the stage angle θ by the following equation, $\Lambda=\lambda_{laser}/2 \sin\theta$, as plotted in Fig. 2.

With the 325 nm wavelength of the HeCd laser, a stage angle of $\theta=45°$ results in $\Lambda=\sim 240$ nm, suitable for 1550 nm based applications, as shown by the right stage in Fig. 1. By rotating the sample and mirror relative to the incident light, the grating pitch can be adjusted. At the limiting incident angle of 90°, the pitch can be reduced to 163 nm, but this is an impractical exposure angle and is unsuitable for gratings at 980 nm.

In order to achieve $\Lambda=\sim 155$ nm necessary for first-order 980 nm Bragg gratings, a shorter incident wavelength must be used in the holography setup. However, we have developed a more elegant solution of reducing the effective wavelength of the HeCd source using a prism. As shown by the left stage in Fig. 1, a prism replaces the conventional mirror stage. The sample is adhered to one side of the prism with xylene, which also acts as an index-matching fluid. The expanded laser beam enters the prism through the hypotenuse face of the prism and standing wave patterns are created

[a]Electronic mail: cswang@engineering.ucsb.edu

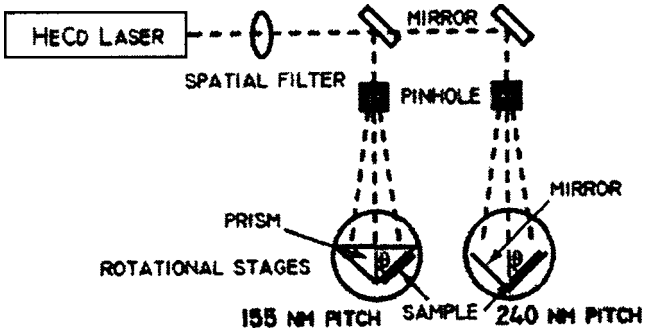

FIG. 1. Schematic of the holography setup. The right stage is used for exposing gratings with ~240 nm pitch. The left stage is used for exposing gratings with ~155 nm pitch through a prism. The sample adheres to the prism by using the index-matching fluid xylene.

from reflections from the two sides of the prism. As shown in Fig. 2, the wavelength of the HeCd source is reduced by $n_{\text{prism}}=1.482$, and the resulting pitch at $\theta=45°$ is ~155 nm. The hypotenuse face of the prism was antireflective coated to prevent unwanted reflections.

To pattern the GaAs wafers, first photoresist was spun onto the samples which were then patterned using the immersion holography technique. Typical exposure energies were 30 mJ. After developing the exposed photoresist, the samples were subjected to a 7 s O_2 plasma ashing to ensure that the semiconductor is clearly exposed at the bottoms of the photoresist gratings. The duty cycle of the gratings can be controlled by the exposure time and power of O_2 plasma ashing. Next, the grating pattern was transferred into the GaAs wafer by using an inductively coupled plasma reactive ion etch with Cl_2-BCl_3-Ar. The target etch depth was 45 nm deep. Figure 3 shows a SEM image of the etched gratings. The gratings are uniform with square shape. Finally, the samples were cleaned for regrowth. The grating pitch can be accurately measured by placing the finished sample back on the prism and measuring the diffraction angle of the incident beam.

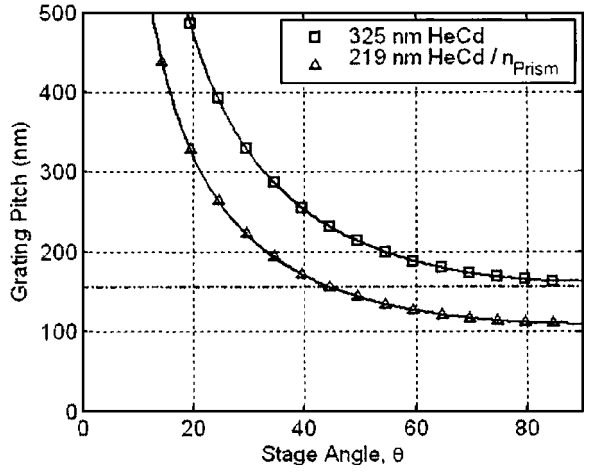

FIG. 2. Grating pitch as a function of stage angle. The HeCd laser source is limited to a minimum pitch of 163 nm. By reducing the wavelength via a prism, a 155 nm pitch is achievable at an angle of ~45°.

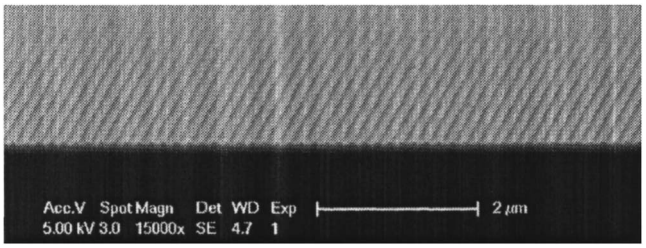

FIG. 3. Scanning electron micrograph of gratings patterned by immersion holography and etched into GaAs.

III. MBE REGROWTH

All growths and regrowths were performed in an ultrahigh vacuum Varian Gen II solid-source MBE system with valved As source. To study the quality of overgrowth on gratings by MBE, the growth rate and growth temperature T_g were varied. The gratings used for these regrowths were fabricated without the use of the prism for simplicity. Gratings were etched into 1 μm GaAs epi templates grown on (100) GaAs substrates. Regions of each sample were covered with Si_xN_y prior to holography and selectively etched in order to obtain both regions with and without gratings. Prior to loading into the MBE chamber for regrowth, the SiN was removed and the samples were subjected to a 1 h UV ozone treatment followed by 30 s 1:2 BHF:DI dip.

Oxide desorption was kept consistent throughout the regrowths. With an As_2 overpressure of 1×10^{-5} (V/III ratio=25), the substrate was heated to a temperature of 620 °C, as measured by an optical pyrometer, upon which (4×2) reconstruction could be seen. The substrate was then held at 625 °C for 2 min before cooling to growth temperature. It was found that holding the substrate hotter or longer resulted in significant surface migration of the GaAs grating tooth, essentially destroying the square grating shape. While not used in this work, including a hydrogen radical cleaning step prior to oxide desorption has been shown to effectively remove oxides and contaminants.[9,10] This would eliminate the need for high temperature thermal oxide desorption to further preserve the grating shape and improve regrowth quality.

Regrowths consisted of first depositing 1 nm of GaAs followed by a 6 nm grade up to $Al_{0.75}Ga_{0.25}As$. After 900 nm of $Al_{0.75}Ga_{0.25}As$, the regrowth finished with a 45 nm grade down to 100 nm of GaAs. Initial regrowths were performed with a V/III ratio of 25. Digital superlattices were used for the AlGaAs which has been found to result in better material quality than compared to analog growth.[8] When regrowing over gratings using growth conditions of 1 μm/h growth rate at $T_g=600$ °C, the resulting epi was rough and had dense pitting defects, as shown in Fig. 4(a). To reduce the pitting defects, the growth rate was slowed and the substrate temperature was varied. Slowing the growth rate has been shown to reduce threading dislocation defects.[8] Similarly, we found that the pitting defect density was reduced for slower growth rates of 0.5 and 0.2 μm/h, as shown in Figs. 4(b) and 4(c). In addition, three substrate temperatures of 585, 600,

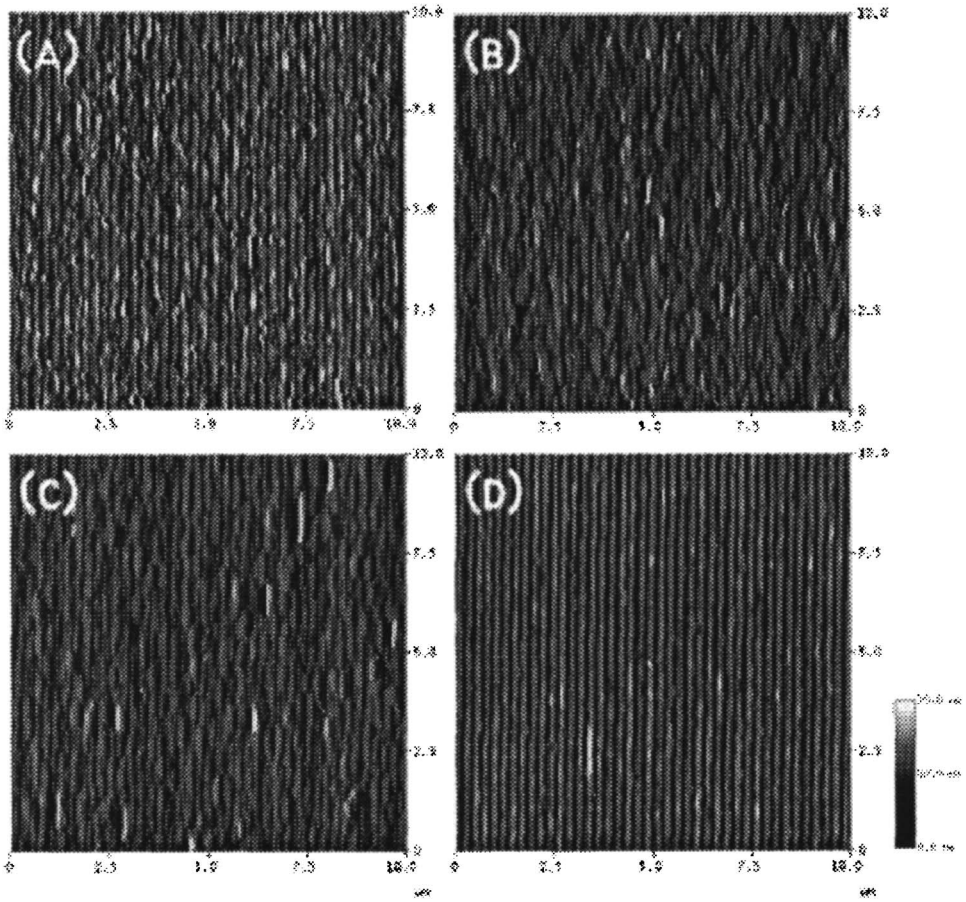

FIG. 4. AFM images of regrown gratings for growths rates of (a) 1 μm/h, (b) 0.5 μm/h, and (c) 0.2 μm/h grown at 600 °C. The sample in (d) is regrown gratings with an initial slow growth rate of 0.2 μm/h at V/III=15, then finished with a 1 μm/h growth rate at V/III=25 grown at T_g =585 °C. 1 μm of $Al_{0.75}Ga_{0.25}As/GaAs$ was regrown over GaAs gratings.

and 615 °C were used to observe the effect of T_g. While not as pronounced, hotter growth temperatures tended to somewhat reduce pitting defects.

While slowing the growth rate and increasing the growth temperature improved growth over grating regions, growth over field regions without gratings became rougher. Field regions grown either at 0.2 μm/h or at 615 °C yielded rms roughness values in excess of 13 Å. It was found that a lower V/III ratio was needed to smooth out the field regions, resulting in rms roughness values of around 3 Å. Lowering the arsenic overpressure did not adversely affect growth over grating regions. The final regrowth condition used was an initial slow growth rate of 0.2 μm/h at T_g=585 °C with a V/III ratio of 15. After 0.5 μm of growth, the cell temperatures were heated and the remainder of the growth occurred at a growth rate of 1 μm/h, also at T_g=585 °C. Figure 4(d) shows an AFM image of regrowth over gratings with the dual growth rate conditions. While the finished growth is not planar, this should not adversely affect the gratings since the surface is significantly far away from the lasing mode. It is more important to note that the pitting defects have been minimized, which would be a larger source of scattering loss.

IV. DEVICE PERFORMANCE

To investigate the performance of the gratings, the gratings were monolithically integrated into a DBR laser structure, with a side-view schematic as shown in Fig. 5. The gain section is 250 μm long; a DBR is used for the rear mirror and a cleaved facet is used for the front mirror. Behind the DBR is active material that serves as a back absorber to prevent reflections back into the cavity.

Complete details of the epitaxial structure and fabrication process can be found in Ref. 2. A centered quantum well structure was used consisting of three InGaAs/GaAs sandwiched between $Al_{0.3}Ga_{0.7}As$ waveguides. A 65 nm GaAs layer above the waveguide serves as the grating and regrowth layer. After patterning and etching gratings using the immersion holography technique, regrowth was performed to overgrow a 1.8 μm thick $Al_{0.75}Ga_{0.25}As$ p cladding. The dual growth rate conditions similar to the one used for Fig. 4(d)

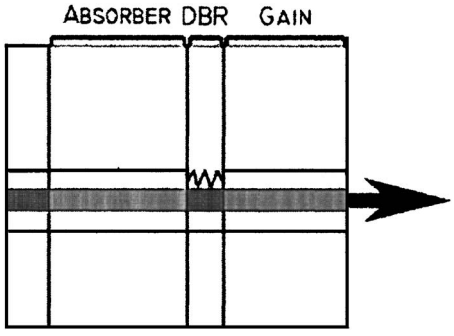

FIG. 5. Side-view schematic of the DBR laser structure.

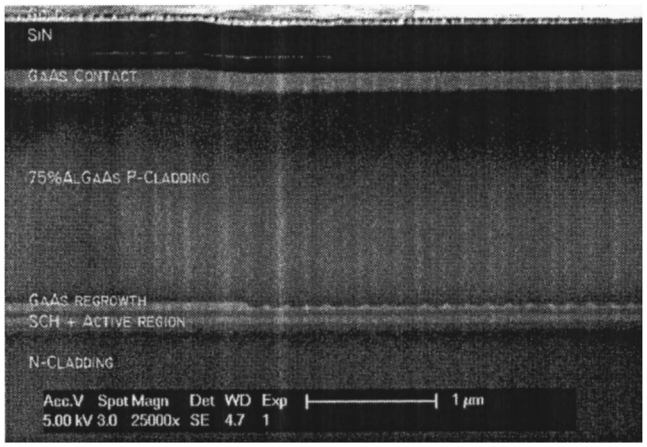

FIG. 6. SEM of regrown laser structure showing both field and grating regions.

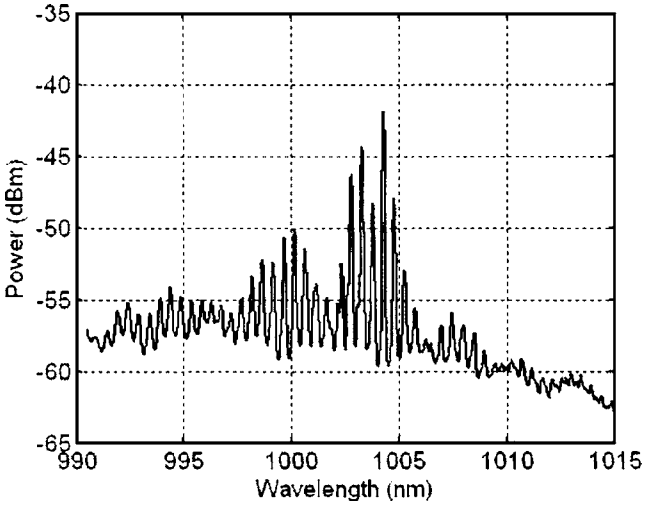

FIG. 8. Subthreshold spectra of the DBR laser biased at $0.98I_{th}$.

were applied for these DBR lasers. Figure 6 shows a SEM of a regrown laser structure, showing both active and grating regions. From the SEM, overgrowth on the gratings has resulted in a somewhat triangular shape. This is most likely due to some diffusion that occurs during the entire regrowth, which has decreased the tooth depth to ~25 nm from a target etch depth of ~40 nm. This slight reduction in κ can be improved by increasing the etch depth and adjusting the duty cycle.

The DBR lasers were tested under continuous wave (cw) operation, and the light and voltage characteristics are plotted in Fig. 7. The devices were operated single mode at 1003 nm with 30 dB side mode suppression, as shown in the inset. A threshold current of 16 mA (J_{th}=2133 A/cm^2) was measured and output powers of 5 mW were achieved with a gain section current of 45 mA.

To calculate the κ of the gratings, the subthreshold spectra of the DBR laser were measured, as shown in Fig. 8. Using the method described by Yee *et al.*, the subthreshold mode spacing was measured to be .49.[11] The simulated effective group index η_{ge} of the laser structure is 3.85. From this, the effective cavity length L_{eff} is 267 μm, which corresponds to a κ of 312 cm^{-1}. From measurements on the SEM, this value is slightly lower than the simulated κ of ~400 cm^{-1} for a triangular shaped grating for a tooth depth of 25 nm. Nevertheless, high-κ gratings have been demonstrated and implemented in a DBR laser structure.

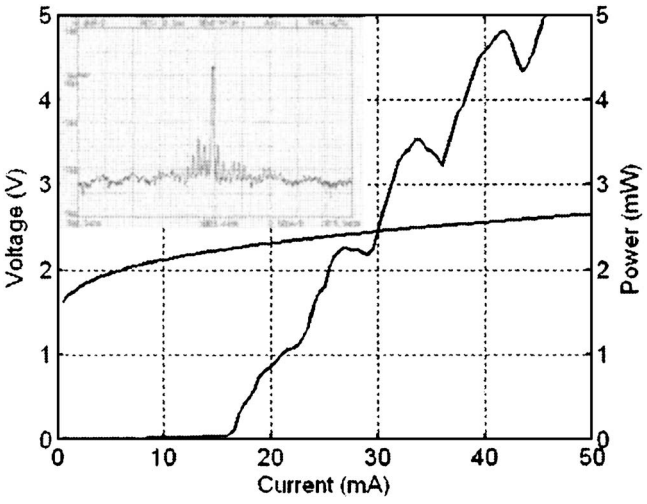

FIG. 7. cw LIV of the DBR laser. The kinks in the power curve are due to mode hops. The inset shows a lasing spectrum of the device biased at $2.5I_{th}$.

V. SUMMARY

In conclusion, first-order, high contrast AlGaAs/GaAs diffraction gratings have been developed and implemented into a DBR laser emitting at 980 nm. An immersion holography technique has been developed to fabricate uniform gratings, and optimum regrowth conditions by MBE were found to overgrow and fill in the gratings. The gratings were successfully integrated in a DBR laser structure resulting in single-mode emission at 1 μm. While initial results of the DBR laser showed relatively low output powers, this could be improved by increasing the injection efficiency of the material. Additional optimization of the epilayer structure could also be made, particularly band engineering the GaAs regrowth layer to eliminate this hole barrier in the laser section and improve the waveguiding for optimal modal overlap with the active region. Further improvements to the gratings could be made by adding additional hydrogen cleaning and adjusting for diffusion during regrowth.

ACKNOWLEDGMENTS

The authors would like to thank the excellent laboratory support of John English. This work was supported by DARPA under the C2OI program. This work made use of MRL Central Facilities supported by the MRSEC Program of the National Science Foundation under Award No. DMR00-80034.

[1]C. S. Wang, E. J. Skogen, J. W. Raring, G. B. Morrison, and L. A. Coldren, *Proceedings of the International Semiconductor Laser Conference* (IEEE, Piscataway, NJ, 2004), pp. 8–9.
[2]G. B. Morrison, C. S. Wang, E. J. Skogen, D. D. Lofgreen, and L. A. Coldren, Proceedings of the Integrated Photonics Research and Applications, San Diego, CA, 2005, Paper No. IWF2.
[3]G. M. Smith, J. S. Hughes, M. L. Osowski, D. V. Forbes, and J. J. Coleman, IEE Electronics Lett. **30**, 651 (1994).
[4]Y. Yuan, T. Brock, P. Bhattacharya, C. Caneau, and R. Bhat, IEEE Photonics Technol. Lett. **9**, 881 (1997).
[5]D. Hofstetter, B. Maisenhölder, and H. P. Zappe, IEEE J. Sel. Top. Quantum Electron. **4**, 794 (1998).
[6]M. Ilegems, H. C. Casey, S. Somckh, and M. B. Panish, J. Cryst. Growth **31**, 158 (1975).
[7]S. Noda, K. Kojima, K. Mitsunaga, K. Kyuma, K. Hamanaka, and T. Nakayama, IEEE J. Quantum Electron. **23**, 188 (1987).
[8]G. W. Pickrell *et al.*, J. Appl. Phys. **96**, 4050 (2004).
[9]T. M. Burke, E. H. Linfield, D. A. Ritchie, M. Pepper, and J. H. Burroughes, J. Cryst. Growth **175/176**, 416 (1997).
[10]H. Künzel, J. Bōttcher, A. Hase, H.-J. Hensel, K. Janiak, G. Urmann, and A. Paraskevopoulos, J. Cryst. Growth **175/176**, 411 (1997).
[11]H. H. Yee, H. T. Hsu, J. Y. Chang, and P. C. Chen, Proc. SPIE **4216**, 103 (2001).